Predictive Dynamic Channel Allocation Scheme for Improving Power Saving and Mobility in BWA Networks

Jenhui Chen · Wei-Kuang Tan

Abstract The radio spectrum of IEEE 802.16 medium access control (MAC) protocol ranges from 2–66 GHz, which is one of potential solutions for broadband wireless access (BWA) or beyond third generation (B3G)/ 4G networks. The maximum transmission range can reach about 48 km. However, with the property of radio propagation, the maximum transmission distance is proportioned inversely to the frequency the mobile subscriber station (MSS) carries. According to this property, the channel allocation can be based on how far the distance between the MSS and the base station (BS) in a macrocell. Therefore, this paper first proposes a new concept of channel allocation model for BWA system and investigates the relations between the signal propagation and the distance as well as propose a signal-aware dynamic channel allocation (SDCA) scheme for dynamic channel allocation (DCA) in BWA networks (BWANs). The SDCA enables the BS to allocate appropriate channels to MSSs according to the received signal-to-noise ratio (SNR) value from the MSSs. Besides, according to the frequency, the SDCA can estimate a minimum power for MSS to communicate. The SDCA not only increases the capacity of the system but saves the overall power consumption of the system well. We also present a new out-of-service prevention scheme for supporting mobility in the system. Simulation results show that the proposed SDCA can achieve the channel utilization (throughput) by up to 94.4% when the spectrum ranges from 2–11 GHz.

J. Chen (✉) · W.-K. Tan
Department of Computer Science
and Information Engineering, Chang Gung University,
Kweishan, Taoyuan, Taiwan, Republic of China
e-mail: jhchen@mail.cgu.edu.tw

Keywords algorithm · broadband · channel allocation · mobility · OFDM · spectrum · wireless

1 Introduction

The frequency allocation method of IEEE 802.16 wireless metropolitan area network (WMAN) standard includes fixed channel allocation (FCA) and dynamic channel allocation (DCA) schemes. FCA follows the initial characteristics of the mobile subscriber station (MSS), e.g., decaying, multipath fading, frequency enhanced ratio, and power, etc. [12], to allot each MSS an exclusive channel in advance. Some performance issues for FCA are studied in [28, 38]. Comparing with FCA, DCA does not reserve exclusive channels for MSSs beforehand, but stands on and follows the characteristics of MSSs to offer proper channels [9]. The potential implementation of DCA has been attracting some interest for years due to the need for larger capacities and more flexibility than those achieved through FCA. Nowadays many DCA schemes are investigated and proposed in various wireless networks [7, 8, 27, 36, 37]. It is well known that DCA algorithms based on measurement of actual interference, i.e., interference adaptive DCA (IA-DCA), perform better than those based on traffic assessment.

Broadband wireless access (BWA) has received much more attentions in recent years [15, 16, 25, 39]. Work towards specification of "beyond third generation" (B3G) or fourth generation (4G) is ongoing [6, 17, 30]. On the path toward 4G, it has to be seen as the next-generation communications system, which may include new wireless access technologies, but in

any case will be able to provide an acceptable broadband access. It can be foreseen that the demand on high bandwidth transmission follows a large number of multimedia applications [23, 35] in wireless communications will be inevitable in the near future.

Fixed BWA systems, such as the local multipoint distribution service (LMDS), provide multimedia services to a number of discrete subscriber sites with IP and offer numerous advantages over wired IP networks. This is accomplished by using base stations (BSs) to provide network access services to subscriber sites based on IEEE 802.16 WirelessMAN standard [11]. The progress of the standard has been fostered by the keen interest of the wireless broadband industry to capture the emerging WiMAX (worldwide interoperability for microwave access) market, the next-wave wireless market that aims to provide wireless broadband Internet services. The WiMAX Forum, formed in 2003, is promoting the commercialization of IEEE 802.16 and the European Telecommunications Standard Institute's (ETSI) high performance radio MANs (HyperMANs). It provides one of potential solutions to B3G/4G architecture [26, 33].

In recent year, a large number of papers in literature dealing with the proposal and/or the performance evaluation of DCA schemes, but only a small number of them are applied for BWA networks (BWANs) correspondingly. With the characteristic of radio propagation, a longer distance will cause fading signal and losing path conspicuously [40] and the signal arriving the BS from the subscriber station with lower frequency will take a longer distance than that of higher frequencies [5]. According to above mentions, with the wide range of spectra (2–66 GHz), thousands of channels will be able to be allocated for access in a cell of BWAN, which we will call a *macrocell* hereafter, if each channel's bandwidth is 20 MHz. How to organize these channels efficiently to increase the maximum capacity of the system has become very important [1, 14]. Thus, in this paper, we first point out the problem of how to efficiently distribute channels (or frequencies) to MSSs according to distances between the MSSs and the BS, and then propose a new macrocell channel arrangement model for BWA's cellular system.

Based on this model, we design a signal-aware DCA (SDCA) scheme to coordinate MSS's channel allocation according to the received signal-to-noise ratio (SNR) value of signal arriving the BS from the MSS. One major benefit of this scheme is that, without global positioning system (GPS) [29], SDCA can estimate the distance of the MSS to the BS by only using the SNR value whether in urban or suburban area. Furthermore, the MSS will be informed by the BS to reduce its trans-

mission power so that the overall power consumption is minimized. Finally, considering the mobility of MSSs in the macrocell, SDCA also supports MSS in various velocities and movements in different directions without out of radio service. We also show that the proposed SDCA not only increases the capacity of the system and the capability of MSS's mobility in BWAN but reduces the call blocking probability by allocating an appropriate channel for MSSs.

This paper is organized as follows. Section 2 takes an overview of the mechanism of IEEE 802.16 MAC protocol. In Section 3, we illustrate the relationship of the measured SNR and maximum transmission distance in detail. Section 4 introduces a new macrocell channel arrangement model and SDCA for IEEE 802.16 networks. In Section 5, we give the performance evaluations of SDCA and show the impact of SDCA to the IEEE 802.16 networks. Finally, some concluding remarks are discussed in Section 6.

2 IEEE 802.16 overview

First published in April 2002, IEEE 802.16 standard has recently been updated to IEEE 802.16-2004 [18] (approved in June 2004). The standard focuses on the "first-mile/last-mile" connection in WMANs. Its purpose is to facilitate the optimal use of bandwidth from 2–66 GHz, as well as interoperability among devices from different vendors. Typical channel bandwidth allocations are 20 or 25 MHz (United Stats) or 28 MHz (Europe) in 10–66 GHz, or various channel bandwidths among 1–30 MHz in 2–11 GHz [19].

IEEE 802.16 has the maximum transmission distance around 1.6–4.8 km and data rate up to 120 Mb/s. It provides a framework of BWA backbone networks based on various BSs. In IEEE 802.16a [19], the transmission distance is expended to 6–10 km with maximum data rate up to 75 Mb/s. It supports nonline-of-sight (NLOS) communications and thus fits in urban environment, which may have a lot of hindrances. Moreover, for the need of mobility in different radio access networks (RANs), IEEE 802.16e [20] is established for roaming of MSSs and operates in frequencies below 6 GHz. The supplied data rate is approximately 15 Mb/s if the channel bandwidth is 5 MHz.

The IEEE 802.16 physical (PHY) layer requires equally radio link control (RLC), which is the capability of the PHY to transition from one burst profile to another. RLC begins with periodic BS broadcast of the burst profiles that have been chosen for the uplink (UL) and downlink (DL). The particular burst profiles used on a channel are chosen based on a number of

factors, such as rain region and equipment capabilities [22, 25]. For ongoing ranging and power adjustments, the BS may transmit unsolicited ranging using ranging response (RNG-RSP) messages commanding the MSS to adjust its corresponding power or timing.

During initial ranging, the MSS requests to be served in the downlink via a particular burst profile by transmitting its choice of downlink interval usage code (DIUC) to the BS. The BS commands the MSS to use a particular uplink burst profile simply by including the appropriate burst profile uplink interval usage code (UIUC) with the MSS's grants in UL-MAP messages. After initial determination of uplink and downlink burst profiles between the BS and a particular MSS, RLC continues to monitor and control the burst profiles. The MSS can use ranging request (RNG-REQ) message to request a change in downlink burst profile. The channel measurements report request (REP-REQ) message shall be used by a BS to request SNR channel measurement reports. The channel measurement report response (REP-RSP) message shall be used by MSS to respond to the channel measurements listed in the received REP-REQ.

The investigated IEEE 802.16a PHY uses orthogonal frequency division multiplexing (OFDM) with 256-point transform, designed for NLOS operation in 2–11 GHz frequency bands, both licensed and license exempt. Time division duplex (TDD) and frequency division duplex (FDD) variants are defined. Typical channel bandwidths vary from 1.25–28 MHz. There are more optional air interface specifications, e.g., based on orthogonal frequency division multiple access (OFDMA) with 2,048-point transform or based on single-carrier modulation. The finalization of IEEE 802.16-2004 standard improves the OFDM technology, which splits a given frequency into subcarriers. This lets operators transmit more signals over a given frequency with less likelihood of interference, a key factor in opening up unlicensed spectrum. IEEE 802.11 has a 64 OFDM physical layer, while IEEE 802.16 features a 256 OFDM architecture.

The IEEE 802.16e [20] is referred to as the process of an MSS scanning and/or ranging one or more BSs in order to determine suitability, along with other performance considerations, for network connection or hand-over, etc. The MSS may incorporate information acquired from an MOB-NBR-ADV message to give insight into available neighboring BS for cell selection consideration [2, 21, 31]. These technologies provide the MSSs with mobility in BWANs.

Although IEEE 802.16 standard defines DL-subframe and UL-subframe that determine the downlink and uplink channel allocation, such as DL-MAP

and UL-MAP, it does not define how to allocate these large channels efficiently for enhancing the maximum capacity of BS and MSSs. In this paper, we will consider the whole above facts to improve the overall capacity of BWANs and prevent the MSS out of service when it is in mobility.

3 The signal estimation

As we discuss above, the maximum transmission distance is proportioned inversely to the frequency MSS carries. By a pre-planned channel allocation model based on this property, the BS can assign a proper channel to an MSS for communication according to the distance between the BS and MSS. The distance can be obtained by using the well-known global positioning system (GPS) [29]. However, applying the GPS will increase the prime cost of the implementation of mobile communication devices and reduce the possibility of implementation to market. Besides, more important, the obtained distance is not sufficient to determine an appropriate channel for allocation since the system still lacks the environment parameters such as the path loss, the multipath fading, the figure noise, and the antenna gain, etc. To overcome this problem, we propose a signal-aware dynamic channel allocation (SDCA) scheme based on the received SNR value of signal arriving the BS from the MSS, which is a measured value from the PHY, to estimate how far the MSS to the BS and select a proper channel for allocation to the MSS.

The power received from a transmitter at a separation distance d directly impacts the SNR, which the desired signal level is represented in received power P_r and is derived by

$$P_r = \frac{P_t G_t G_r}{\mathrm{PL}(d) L} \text{ [Valid if } d \gg 2D^2/\lambda], \quad (3.1)$$

where P_t is the transmitted power, G_t and G_r are the transmitter and receiver antenna gains, $\mathrm{PL}(d)$ is the path loss (PL) with distance d, L is the system loss factor ($L \geq 1$, transmission lines etc., but not due to propagation), D is the maximum dimension of transmitting antenna, and λ is the corresponding wavelength of the propagating signal [34]. The measurement unit of P_r is milliwatt (mW). The antenna gain G is equal to $4\pi A_e/\lambda^2$; A_e is the effective aperture of antenna. The length of λ can be obtained by $c/f = 3 \times 10^8/f$ in meters where f is the frequency the signal carries. Besides, the P_r can be represented in dBm units as

$$P_r[\mathrm{dBm}] = 10 \log(P_r[\mathrm{mW}])$$
$$= P_t + G_t + G_r - \mathrm{PL}(d) - L. \quad (3.2)$$

In the free space propagation model, the propagation condition is assumed idle and there is only one clear line-of-sight (LOS) path between the transmitter and receiver. On unobstructed LOS path between transmitter and receiver, the PL can be evaluated as

$$PL(d) = \frac{(4\pi)^2 d^2}{\lambda^2} \quad (3.3)$$

or when powers are measured in dBm units

$$PL(d) = 92.4 + 20\log(f) + 20\log(d). \quad (3.4)$$

From Eq. 3.3, we can get the desired T-R separation distance in meters

$$d = \frac{\lambda}{4\pi}\sqrt{PL(d)} = \frac{c}{4\pi f}\sqrt{PL(d)}. \quad (3.5)$$

However, different modulation schemes such as quadrature phase shift keying (QPSK), 16 quadrature amplitude modulation (16-QAM), or 64-QAM have different maximum PL values [33]. These values are 125 dB for QPSK, 120 dB for 16-QAM, and 115 dB for 64-QAM, and will impact the calculations of distance. Figure 1, obtained from Eq. 3.5, shows the relation of the frequency and the distance between two isotropic antennas with different modulation schemes. We can see that a higher frequency will lead to a shorter transmission distance and vice versa. Furthermore, a higher modulation scheme such as 64-QAM requires lower PL ratio and thus achieves an overall shorter transmission distances than lower modulation schemes if the transmission power is fixed.
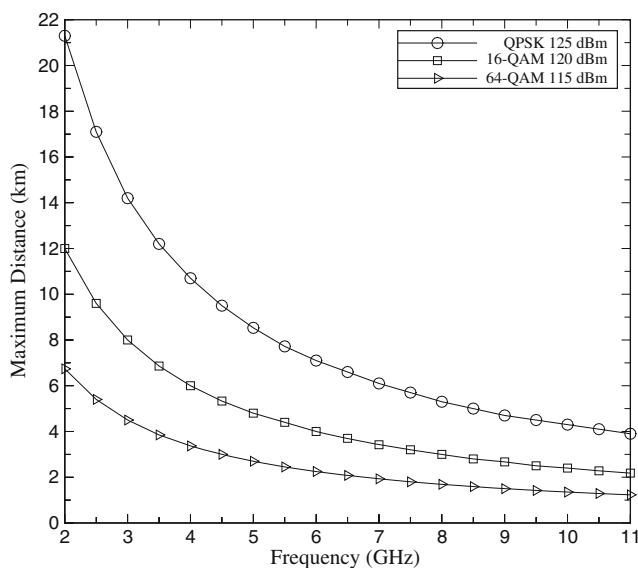

Fig. 1 Maximum transmission distance versus frequency domains from 2 to 11 GHz in OFDM with different modulation schemes

Nevertheless, this equation can not be applied in street canyon scenario or urban environment. A general PL model that has been demonstrated through measurements uses parameter σ to denote the rule between distance and received power [3]. $PL(d)$ in realistic environment can be expressed as

$$PL(d) = PL(d_0) + 10\rho\log\left(\frac{d}{d_0}\right)$$
$$+ X_\sigma + C_f + C_H; \quad d \geq d_0, \quad (3.6)$$

where the term $PL(d_0)$ is for the free-space PL with a known selection in reference distance d_0, which is in the far field of the transmitting antenna (typically 1 km for large urban mobile system, 100 m for microcell systems, and 1 m for indoor systems) and is measured by $PL(d_0) = 20\log(4\pi d_0/\lambda)$. X_σ denotes a zero-mean Gaussian distributed random variable (with units in dB) that reflects the variation in average received power that naturally occurs when PL model of this type is used [13]. ρ is the path loss exponent, where $\rho = 2$ for free space, and is generally higher for wireless channels. It can measured by $\rho = (a - bH_b + c/H_b)$, where a, b and c are constants for each terrain category. The numerical values for these constants is studied in [12] where H_b is the height of the base station and is $10 \text{ m} \leq H_b \leq 80 \text{ m}$. C_f is the frequency correction factor, accounts for a change in diffraction loss for different frequencies which a simple frequency dependent correction factor C_f due to the diffraction loss, and measured by $C_f = 6\log(f/1900)$ [10]. C_H is the receiver antenna height correction factor and h is the receiver antenna height. $C_H = -10.7\log(h/2)$ when $2 \text{ m} \leq H \leq 8 \text{ m}$. This correction factor closely matches the Hata–Okumura mobile antenna height correction factor for a large city [14]. The mostly NLOS conditions, doubling the receiver antenna height results in approximately 3.5 dB decrease in path loss.

As we know that the audio or video quality of a receiver is directly related to the SNR; the greater the SNR is, the better the reception quality is. The limiting factor on a wireless link is the SNR required by the receiver for useful reception

$$SNR(dB) = P_r(dBm) - N_0(dBm), \quad (3.7)$$

where $N_0(dBm)$ is the noise power in dBm. Assume the carrier bandwidth is B, the receiver noise figure is F, the spectral efficiency is r_b/B, and the coding gain is G_c. Then the SNR for coded modulation with data rate r_b can be obtained by

$$SNR(dB) = 10\log\left(\frac{P_r}{N_0} \cdot \frac{r_b}{B}\right) - G_c, \quad (3.8)$$

where

$$N_0(\text{dBm}) = -174(\text{dBm}) + 10 \log B + F(\text{dB}) \qquad (3.9)$$

and G_c is normally considered as 5 dB. The noise might consist of thermal noise generated in the receiver, co-channel or adjacent channel interference in frequency division or time division multiple access systems, or multiple access interference in code division multiple access spread spectrum systems.

4 The signal-aware dynamic channel allocation scheme

4.1 The measured SNR

As we discuss the SNR value in previous section, the SNR value is affected by the transmitted power and the frequency it carries. In order to obtain a criterion measurement of the received SNR, we enforce each MSS which has packets to transmit has to use the lowest frequency to contend the channel access right during the uplink contention period with a pre-defined transmission power. The reason we consider the channel of lowest frequency as the *contention channel* is that we want to ensure that each MSS can communicate with the BS even if it is in the boundary of the macrocell since the lowest frequency can get the maximum transmission distance.

The BS, after receiving a RNG-REQ message from the MSS, calculates the estimated distance between the BS and MSS according to the received SNR value. Assume the BS needs a necessary received minimum power or sensitivity $P_{r,\min}$ from each MSS, which corresponds to a minimum required SNR value denoted as $\text{SNR}_{r,\min}$, to successfully receive the signal. Then, according to Eqs. 3.2 and 3.7, we have

$$\text{SNR}_{r,\min} = P_{r,\min} - N_0$$
$$= P_t + G_t + G_r - \text{PL}(d) - L - N_0. \qquad (4.1)$$

Substituting Eq. 3.6 in Eq. 4.1 leads to

$$\text{SNR}_{r,\min} = P_t + G_t + G_r - 20 \log\left(\frac{4\pi d_0 f}{c}\right)$$
$$- 10\rho \log\left(\frac{d}{d_0}\right) - X_\sigma$$
$$- C_f - C_H - L - N_0$$

$$\Rightarrow 10\rho \log\left(\frac{d}{d_0}\right) = P_t + G_t + G_r - 20 \log\left(\frac{4\pi d_0 f}{c}\right) - X_\sigma$$
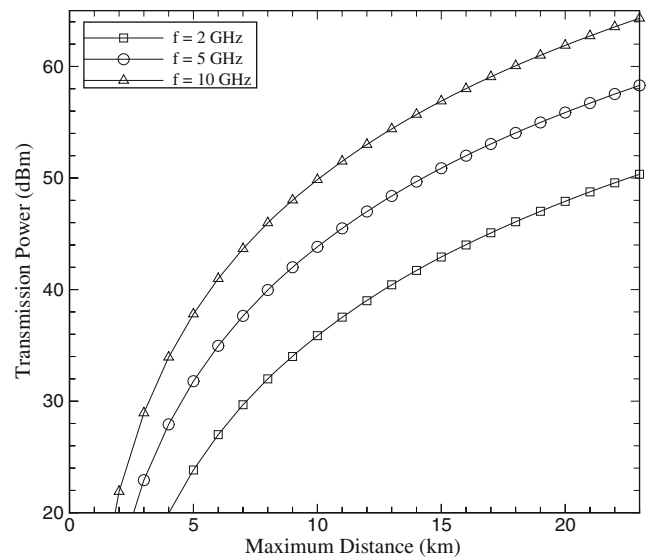$$- C_f - C_H - L - \text{SNR}_{r,\min} - N_0. \qquad (4.2)$$

Fig. 2 Transmission power versus maximum distance when $\rho = 4$, $B = 20$ MHz, coding rate = 3/4, $\text{SNR}_{r,\min} = 24.4$ dB, $F = 7$, $G_t = 16$, $G_r = 18$, $L = 5$ dB

Solving Eq. 4.2 for maximum transmission distance d denoted as $d_{\max}$, then we have

$$d_{\max} = d_0 \times 10 \exp\left\{\left[P_t + G_t + G_r - 20 \log\left(\frac{4\pi d_0 f}{c}\right)\right.\right.$$
$$\left.\left. - X_\sigma - C_f - C_H - L - \text{SNR}_{r,\min} - N_0\right]/10\rho\right\}. \tag{4.3}$$

In the following, for instance, we use the 64-QAM modulation scheme to show the relationship among P_t, $d_{\max}$, and $\text{SNR}_{r,\min}$, respectively. Figure 2 shows the comparisons of P_t with $d_{\max}$ in detail. We can see that the required P_t is proportionally increasing with $d_{\max}$. Meanwhile, a lower frequency, 2 GHz in this example, will get lower power consumption than that of higher frequencies. This implies that the power consumption can be further minimized if the MSS adjusts P_t according to the assigned channel to its current geographical location.

Figure 3 compares $d_{\max}$ with different f under different ρ when applying a fixed P_t, G_t, and G_r. We can see that higher f will lead to shorter $d_{\max}$ and vice versa. We also note that $d_{\max}$ will be shorter when in urban environment (higher ρ). This implies that the scale of the macrocell is affected by different areas and can be adjust by system operators according to the environment. Figure 4 shows the comparison of $d_{\max}$ with the measured $\text{SNR}_{r,\min}$ of the BS. When vary the $\text{SNR}_{r,\min}$ of the receiver, the achievable $d_{\max}$ will proportionally decrease with increasing the required
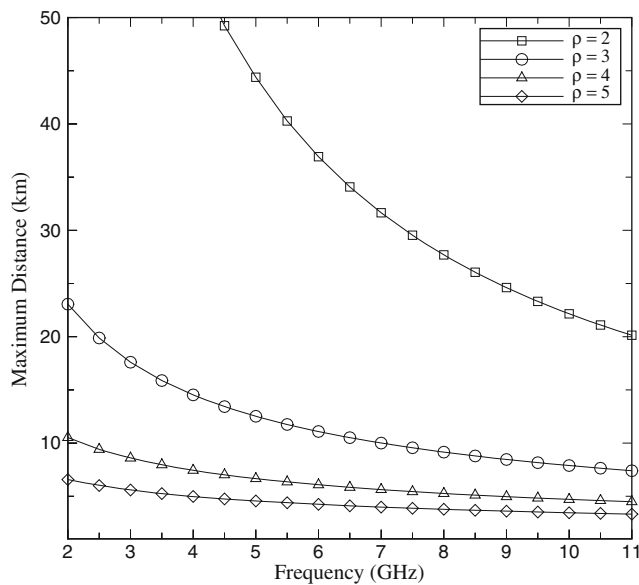
Fig. 3 Maximum transmission distance versus frequency when $B = 20$ MHz, coding rate $= 3/4$, $SNR_{r,\min} = 24.4$ dB, $F = 7$, $G_t = 15$, $G_r = 18$, $P_t = 16$ W, $L = 5$ dB

$SNR_{r,\min}$. The $d_{\max}$ can also be achieved by adopting a higher sensitive receiver of the BS.

4.2 Channel provisioning

Now we want to solve how to determine the scale of a macrocell and allocate channels in the macrocell accordingly, which can reflect the actual size of each section in the macrocell. Assume k independent discrete spectrum sections are available in a marcocell and
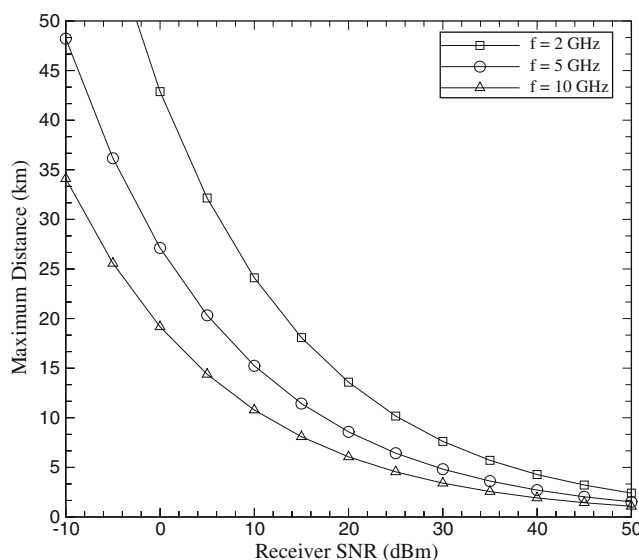

Fig. 4 Maximum distance versus receiver SNR when $\rho = 4$, $B = 20$ MHz, coding rate $= 3/4$, $F = 7$, $G_t = 16$, $G_r = 18$, $P_t = 15$ W, $L = 5$ dB

are represented as $S_1, S_2, \ldots, S_k$. The total available bandwidth of these spectra will be $S = S_1 + S_2 + \ldots + S_k = \sum_{i=1}^{k} S_i$. If each channel has bandwidth B, the available number of channels in each spectrum section is given by

$$n_i = \left\lfloor \frac{S_i}{B} \right\rfloor, \ i \in \{1, 2, \ldots, k\}. \tag{4.4}$$

Thus, we have a total number of available channels $N = \sum_{i=1}^{k} n_i$ for usage.

Assume the BS has the omnidirectional antenna and a number of MSSs M are randomly distributed in a macrocell. Before assigning channels to the macrocell, we have to determine how to allocate an efficient number of channels for utilization according to the fraction of related measure of area so that each area has enough number of channels for use. Assume the macrocell is divided into h concentric circles and the width of each section created by these concentric circles is w as shown in Fig. 5. Thus the area size of the ith concentric circle $D_i = (iw)^2 \pi$ and the area size of the ith section denoted as A_i is given by

$$
\begin{aligned}
A_i &= D_i - D_{i-1} \\
&= (iw)^2 \pi - [(i-1)w]^2 \pi \\
&= (iw)^2 \pi - \sum_{j=1}^{i-1} A_j \\
&= (2i - 1)\pi w^2. \tag{4.5}
\end{aligned}
$$

For example, the area size of $A_2 = (2 \times 2 - 1)\pi w^2 = 3\pi w^2$ and $A_3 = 5\pi w^2$. From Eq. 4.5, we can observe that the ratio of the ith section's area size to the first section's area size is $A_i = (2i - 1)A_1$.

Suppose MSSs are randomly and normally distributed in the macrocell, the channel allocation can follow the ratio of A_i to A_1 accordingly. Consequently, the number of channels in each A_i denoted as C_i will be $(2i - 1)C_1$. According to the characteristic of transmission distance increasing proportionally with a decreasing frequency, we allocate available channels in accordance with the highest to the lowest frequency channels from the inner to the outer side of the macrocell. Then we have $C_1, C_2, \ldots, C_h$ and $C_2 = 3C_1$, $C_3 = 5C_1$ and so forth as shown in Fig. 5.

However, MSSs in the outer side of the macrocell will lead to the co-channel effect with other outer sides of neighboring macrocells if we allocate same frequencies in the A_h. To tackle this problem, we reserve three times C_h for allocation in different neighboring macrocells so that neighboring A_h will have different frequencies for transmission as shown in Fig. 6.
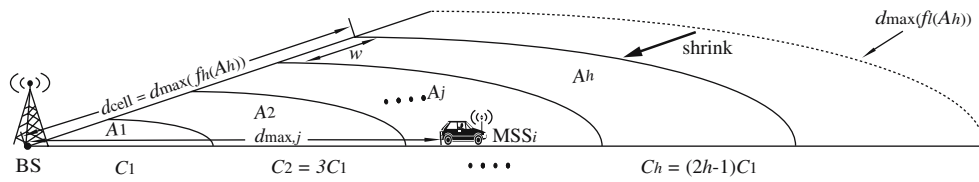
Fig. 5 An illustration of channel arrangement within the macrocell. The channel allocation is from highest frequency to lowest frequency and is started from the inner side of the marcocell (the *left side* of the figure)

Deducting the contention channel ($C_0 = 1$) from N, the allocated channels satisfy

$$C_1 + C_2 + \ldots + C_{h-1} + 3C_h \leq N - 1 \qquad (4.6)$$

To solve Eq. 4.6 for h, we have

$$\sum_{i=1}^{h} C_i + 2C_h = \left\{ \sum_{i=1}^{h} (2i-1) + 2(2h-1) \right\} C_1 \leq N-1$$

$$\Rightarrow \left\{ \frac{[1+(2h-1)]h}{2} + 2(2h-1) \right\} C_1 \leq N-1$$

$$\Rightarrow (h^2 + 4h - 2)C_1 \leq N - 1$$

$$\Rightarrow h \leq \sqrt{\frac{N-1}{C_1} + 6} - 2, \qquad (4.7)$$

and the upper bound of h is equal to

$$h = \left\lfloor \sqrt{\frac{N-1}{C_1} + 6} - 2 \right\rfloor. \qquad (4.8)$$

Now we have another problem to solve, that is, how long the radius of a macrocell d_{cell} will be. According to Eq. 4.3 and the environment's parameters, we can determine $d_{\max}$ as the d_{cell} easily. However, considering the mobility of MSSs, the MSS may move out the radio service range and lead to out-of-service effect if channels are allocated from higher to lower frequencies and started from the inner side of the macrocell. To overcome this problem, we use $d_{\max}$ of the highest frequency of the A_h denoted as $f_h(A_h)$ as the macrocell's radius. The $f_h(A_h)$ can be obtained by

$$f_h(A_h) = f_{\text{high}} - \left((h-1)^2 C_1 + 1 \right) B, \qquad (4.9)$$

Fig. 6 An illustration of the co-channel problem in SDCA scheme where the number of each macrocell is denoted as a different identification of C_h, which is reserved to avoid interference and co-channel effect with each other
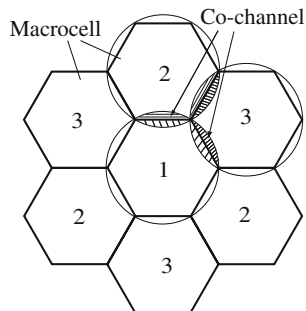
where f_{high} is the highest frequency of the system and $((h-1)^2 C_1 + 1)B$ is the summation of allocated channels' bandwidth from A_1 to A_{h-1}. Substituting Eq. 4.9 in Eq. 4.3, we can have the boundary of macrocell d_{cell} as

$$d_{\text{cell}} = d_0 \times 10 \exp \left\{ \left[P_{\text{ini}} + G_t + G_r \right. \right.$$
$$\left. - 20 \log \left[\frac{4\pi d_0 \left(f_{\text{high}} - \left((h-1)^2 C_1 + 1 \right) B \right)}{c} \right] \right.$$
$$\left. \left. - X_\sigma - C_f - C_h - L - \text{SNR}_{r,\min} - N_0 \right] / 10\rho \right\}, \qquad (4.10)$$

where P_{ini} is the given initial power and also the maximum power of the MSS for estimation of the distance between the BS and the MSS.

We note that the boundary of the macrocell now is shrunk from $d_{\max}(f_l(A_h))$ to $d_{\max}(f_h(A_h))$, see the righthand side of Fig. 5, to avoid out-of-service effect. The reason we use $f_h(A_h)$ to determine the boundary of the macrocell is that the MSS may not reach the BS as it appears near the boundary of the macrocell if it uses the assigned frequency $f_l(A_h) \leq f_a < f_h(A_h)$ with P_{ini} and the boundary is determined by $f_l(A_h)$. According to this plan, it is guaranteed that, with f_a and P_{ini}, every MSS in A_h can communicate with the BS.

Following above discussions, the boundary of each A_j is determined by $f_h(A_j)$, e.g., the boundary of A_h is $d_{\max}(f_h(A_h))$, the boundary of A_{h-1} is $d_{\max}(f_h(A_{h-1}))$, and so forth. As mentioned prior, the macrocell is divided into h sections with equal width w. According to Eq. 4.8, the width of each section w can be obtained by

$$w = \frac{d_{\text{cell}}}{h}. \qquad (4.11)$$

Assume a MSS i wants to communicate with the BS, it first sends a RNG-REQ message to the BS with P_{ini} in the contention channel C_0. The BS, after receiving the request message and the measured $\text{SNR}_{r,\min}$, will

Fig. 7 An illustration of maximum transmission distance under different frequencies with a same initial power P_{ini}. Notice that the '$*$' implies AND
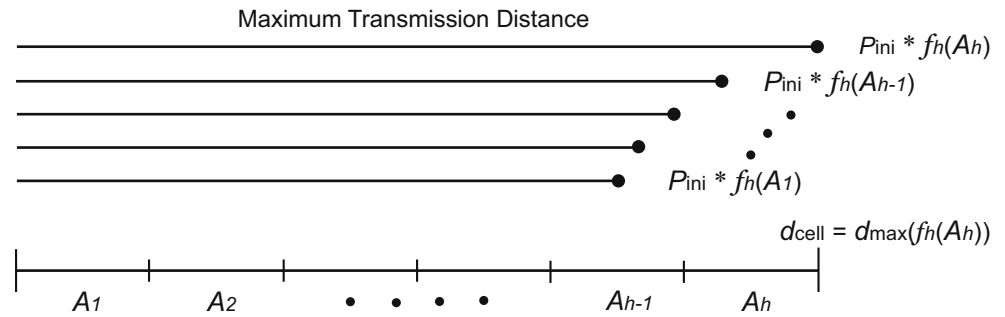
estimate $d_{\text{max},i}$ according to Eq. 4.3. The MSS i can be determined in the jth section by the following equation:

$$j = \left\lceil \frac{d_{\text{max},i}}{w} \right\rceil. \tag{4.12}$$

Although, according to Eq. 4.3, d_{max} increases exponentially by lowering the carried frequency as shown in Figs. 2 and 4. The shortest distance determined by highest frequency with the given power P_{ini} is still more than several kilometers. Figure 7 illustrates the relationship between the achieved $d_{\text{max}}(f_h(A_j))$ with P_{ini} and the corresponding A_j. This result implies that the transmission power can be further reduced after the channel (frequency) is assigned to the MSS.

From Eqs. 4.1 and 4.2, the minimum transmission power $P_{t,\text{min}}$ of the MSS i can be determined by

$$\begin{aligned} P_{t,\text{min}} = \ & \text{SNR}_{r,\text{min}} + N_0 + \text{PL}(d) + L \\ = \ & \text{SNR}_{r,\text{min}} + N_0 - G_t - G_r + 20 \log\left(\frac{4\pi d_0 f_a}{c}\right) \\ & + 10\rho \log\left(\frac{d_{\text{max},i}}{d_0}\right) + X_\sigma + C_f + C_h + L. \end{aligned}$$

$$\tag{4.13}$$

In order to ensure that all channels allocated in A_j can be operated well, the $d_{\text{max},i}$ is set as the boundary of the location the MSS resides and is equal to jw. This assumption can be guaranteed by the following theorem.

Theorem 1 *In any section A_j, all frequencies $f_a \in A_j$ with the $P_{t,\text{min}}$ can reach the boundary of A_j.*

Proof From Eq. 4.13, the $P_{t,\text{min}}$ of the boundary of A_j is determined by highest frequency $f_h(A_j) \in f_a$ and the distance jw. Since the highest frequency $f_h(A_j)$ with power $P_{t,\text{min}}$ can reach the boundary of A_j, all frequencies $f_a \leq f_h(A_j)$ with $P_{t,\text{min}}$ can reach the boundary of A_j.

Once the channel C_1 is determined, channels of each section A_j will be determined accordingly. However, how to determine the size of C_1 is an open issue for discussion. From Eq. 4.8, we have $h \propto 1/C_1$, that is, h will be smaller if C_1 is set larger. This will lead to bigger sections in the macrocell and, unfortunately, get unprecise frequency allocation since a bigger section will have more frequencies for allocation. And all frequencies refer to the same boundary of the section. This drawback would not save the power consumption efficiently. On the contrary, if we set a smaller C_1, h will be larger (w will become smaller) and MSSs may easily across the boundary of sections. This would lead to increase the probability of out-of-service and decrease the user satisfaction.

Besides, some lower frequencies might be remained for dynamic channel resolution usage if there exists the case according to Eq. 4.8. These remaining channels C_B are dynamically allocated to any section A_j of the macrocell as all channels of A_j are not available. These lower frequencies can be treated as reserved channel for backup use.

4.3 Co-channel problems

According to Eq. 4.11, the width of each section is obtained by $w = d_{\text{cell}}/h$. If the w is greater than or equal to $d_{\text{cell}}(1 - \cos 30°)$, see Fig. 8 for details, the second outer section will overlap the neighbor's second outer section. To avoid this problem, w must satisfy

$$w = \frac{d_{\text{cell}}}{h} \geq d_{\text{cell}}(1 - \cos 30°). \tag{4.14}$$

Solving Eq. 4.14 for h, we have

$$h \leq 2(2 + \sqrt{3}) \simeq 7.4641. \tag{4.15}$$

Since h must be an integer, then $h \leq 7$. According to the result, we conclude that when $h > 7$, it will lead to the second or other outer sections co-channel effect. Therefore, from Eq. 4.8, we have $h = \left\lfloor \sqrt{\frac{N-1}{C_1} + 6} - 2 \right\rfloor \leq 7$ and, then, we obtain $C_1 \geq (N-1)/75$. Thus, the
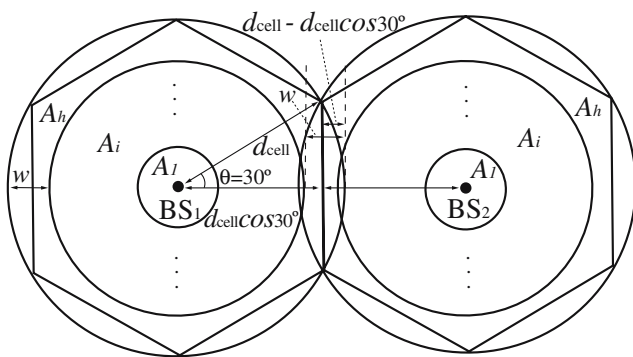
Fig. 8 An illustration of co-channel effect by inner section of neighbor BSs

Fig. 9 An illustration of interference by inner section of neighbor BSs

co-channel effect can be guaranteed only in the most outer section if we make the restriction of $C_1 \geq (N-1)/75$.

Moreover, in the SDCA framework, there still exists another slight problem. This problem, for example shown in Fig. 9, will happen when the MSS_A uploads to the BS_1 and the MSS_B downloads from the BS_2 at the same time if the MSS_A and MSS_B use the same frequency concurrently. The probability of this case is small because it happens just when the MSSs approach the boundary of the A_h and the downloading station MSS_B uses the same channel with MSS_A. To avoid this situation, we have two possible solutions: (1) The BS should detect the channel interferences and select the lowest interference channels to MSSs before assignment; or (2) the superframe is synchronized with its neighboring BSs, that is, all BSs' uplink and downlink are operated at the same time. The latter approach can be easily achieved by coordination among BSs.

Figure 10 shows the proposed SDCA algorithm in detail. Let R_i^{cb} represent the transmission request from MSS i on channel c with request bandwidth b and the total request set $\mathcal{R} = \{R_{i1}^{cb}, R_{i2}^{cb}, \ldots, R_{im}^{cb}\}$. Assume the channel set $\mathcal{C} = \{c_1, c_2, \ldots, c_n | 1 \leq n \leq N\}$ and its precedent occupied bandwidth of c_n is denoted as b_n where $0 \leq b_n \leq B$. The time complexity of the SDAC is $O(n)$ where $n = (2j-1)C_1$ is the number of channels in A_j. This implies that the SDAC is easy to be implemented and can select a channel for MSS rapidly.

4.4 The mobility

In the following, we will discuss the mobility of the MSS in detail. To prevent the out-of-service effect of MSSs due to mobility, we investigate a location prediction scheme to add to SDCA for channel migration. IEEE 802.16 standard recommends that the BS has to broadcast a REP-REQ message to all MSSs for channel measurements within 10 s to check whether the MSS
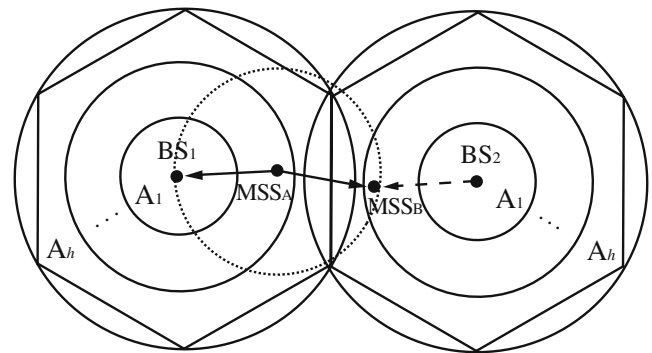
is still in the service set. Therefore, the BS can get the SNR value by the replied REP-RSP message from each MSS to estimate the distance periodically.

Thus, shown in Fig. 11, the movement distance between time t_1 and t_2 of MSS i denoted as $\Delta d_i(\Delta t)$ can be calculated by using cosine theorem as

$$\Delta d_i(\Delta t) = \sqrt{d_{i,t_1}^2 + d_{i,t_2}^2 - 2d_{i,t_1}d_{i,t_2}\cos\theta_{t_2}}, \qquad (4.16)$$

where the θ_{t_2} can be estimated by using smart antenna systems [24, 32] that employ antenna arrays coupled with adaptive signal-processing techniques at the BS. From Eq. 4.16, the average velocity v_i of the MSS i is given by $v_i = \Delta d_i(\Delta t)/\Delta t = \Delta d_i(\Delta t)/(t_2 - t_1)$.

To predict the maximum distance between the MSS i and the BS in time t_3 denoted as t_3', where $t_3' = t_2 + \Delta t$, we have to obtain the ϕ_{t_1}. According to cosine theorem, the ϕ_{t_1} is obtained by

$$\phi_{t_1} = \cos^{-1}\left(\frac{d_{i,t_1}^2 + (\Delta d_i(\Delta t))^2 - d_{i,t_2}^2}{2d_{i,t_1}\Delta d_i(\Delta t)}\right). \qquad (4.17)$$

We simply suppose that each MSS moves forward directly. Then the moving distance can be estimated as

SIGNAL-AWARE DYNAMIC CHANNEL ALLOCATION

BEGIN
    if receive a R_i^{cb} with measured $SNR_{r,\min}$ from MSS i **then**
        estimate the $d_{\max,i}$ and refer to its correspondent A_j;
        check all channels c_n in A_j from high to low frequency;
        if $b_n + b_i \leq B$ **then**
            allocate c_n for MSS i;
            $b_n \leftarrow b_n + b_i$;
        endif
        if cannot find an available channel **then**
            random select a channel for allocation;
        endif
    endif
END

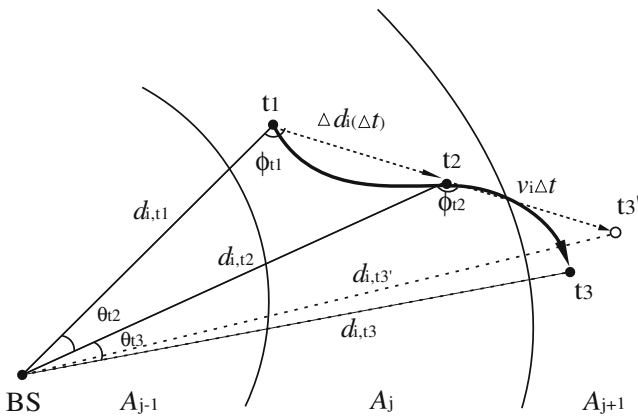
Fig. 10 The algorithm of SDCA in the BS.

Fig. 11 An illustration of mobility

$\Delta d'(t_3 - t_2) = \Delta d(\Delta t) = v_i \Delta t$. Therefore, the estimated distance at time t'_3 will be

$$
d_{i,t'_3} = \sqrt{d_{i,t_1}^2 + \left(\Delta d_i(\Delta t) + v_i \Delta t\right)^2}
$$
$$
- \sqrt{2 d_{i,t_1} \left(\Delta d_i(\Delta t) + v_i \Delta t\right) \cos \phi_{t_1}}. \tag{4.18}
$$

Substituting Eq. 4.17 in Eq. 4.18 we have

$$
d_{i,t'_3} = \Bigg(d_{i,t_2}^2 + 2 v_i \Delta t \sqrt{d_{i,t_1}^2 + d_{i,t_2}^2 - 2 d_{i,t_1} d_{i,t_2} \cos \theta_{t_2}}
$$
$$
- \frac{2 v_i \Delta t d_{i,t_1} (d_{i,t_1} - d_{i,t_2} \cos \theta_{t_2})}{\left(d_{i,t_1}^2 + d_{i,t_2}^2 - 2 d_{i,t_1} d_{i,t_2} \cos \theta_{t_2}\right)^{1/2}}
$$
$$
+ (v_i \Delta t)^2 \Bigg)^{1/2}. \tag{4.19}
$$

Once the predicted distance $d_{i,t'_3} \geq jw$, i.e., the MSS might exceed the boundary of A_j, or $d_{i,t'_3} \leq (j-1)w$, i.e., less the boundary of A_j, the BS will notice the MSS i to migrate to a new channel in A_k ($k = \lceil d_{i,t'_3}/w \rceil$) with the message (P'_t, c'_n). Therefore, by using the prediction to prevent the out-of-service effect, the performance of the BWA system can be maintained well. Besides, the overhead of prediction will not be heavy since we only use the routine procedure of channel measurement, which is specified in the IEEE 802.16 standard, to get the information for estimation.

5 Simulation model and results

5.1 Simulation model

In this section, we design a detailed simulation model for performance evaluation as described below. We adopt IEEE 802.16 as the data link layer protocol and the 64-QAM modulation model with 3/4 coding rate.

The channel bandwidth is considered as 5 MHz and operates in TDD mode. The frame length is set to 20 ms and each OFDM symbol time is evaluated a cyclic prefix of 1/4 of the useful time T_b and is chosen to deal with delay spread values for NLOS operation in suburban areas. We assume P_{ini} of the BS is 300 mW and $P_{t,max}$ of each MSS is limited to 450 mW. Other simulations parameters can be found in Table 1.

There are 1,800 channels ranged from 2 to 11 GHz. The simulation model is composed by three different simulation scenarios. The first scenario has a fixed size of macrocell and its radius is 4.35 km long, which is calculated from $P_t = 300$ mW, $B = 5$ MHz, $C_1 = 24$, $f_h(A_h) = 6.675$ GHz, $\rho = 4$, and $w = 621$ m. In the second scenario, there are 38 channels ranged in the spectrum from 2.5–2.69 GHz and the radius of the BS is 5.228 km long determined by $P_{ini} = 300$ mW and $f_h(A_h) = 2.64$ GHz. The width w of each section is 1,307 m long and h equals 4. In the last scenario, we adopt two segments of spectra 2.5–2.69 GHz and 5.725–5.85 GHz simultaneously. There are totally 63 channels used for channel allocation. The related parameters are $P_t = 300$ mW, $B = 5$ MHz, $C_1 = 1$, and $f_h(A_h) = 5.72$ GHz, respectively. The size of macrocell is 4,675 m, $w = 779$ m, and $h = 6$.

All MSSs are randomly distributed in the macrocell through all simulations. The MAC service data unit (MSDU) arrival rate of each MSS follows the Poisson distribution with a mean λ, which consists of a upload $\lambda_u = 50$ frames/s (0.75 Mb/s) and a download $\lambda_d = 50$ frames/s. That is, each allowed MSS will occupy total 1.5 Mb/s bandwidth including the uplink and downlink transmissions. Each frame length is an exponential distribution with a mean of 1,885 bytes

Table 1 System parameters in simulations

Parameters	Value
Frame length	20 ms
Bandwidth (B)	5 MHz
F_s/B	7/6
$F_s = 7/6 \cdot 20$	5.833 MHz
(T_g/T_b)	1/4
$T_b = 256/F_s$	43.89 μs
OFDM symbol time, $T_{sym} = T_g + T_b$	54.86 μs
Modulation/code rate	64-QAM 3/4
Carriers N_{FFT}	256
Bit rate	15.75 Mb/s
$SNR_{r,min}$	24.4 dB
Tx antenna gain (G_t)	16 dB
Rx antenna gain (G_r)	18 dB
The system loss factor (L)	5 dB
Receiver noise figure (F)	7 dB

($\approx$ 20 ms), which consists of a 6-octets MAC header, a 32-bit cyclic redundancy check (CRC), and a 1,875-octet MSDU payload. The MAC frame consists of four initial maintenance opportunities (UIUC=2) slots, ten request contention opportunities (UIUC=1) slots. The transmit to receive (T_x/R_x) transition gap (TTG) and the R_x/T_x transition gap (RTG) are both 5.14 μs.

5.2 Simulation results

To compare with SDCA, a randomly dynamic channel allocation (RDCA) scheme [18] and measured dynamic channel allocation (MDCA) scheme [41] are simulated for comparison. Figure 12 shows the average P_t of MSSs by varying M in SDCA and RDCA, respectively. From Fig. 12, we can see that SDCA only consumes 53.52% P_t than MDCA and RDCA when $M = 16,000$. This is because that RDCA adopts random fashion to allocate channels for MSSs and may choose higher frequencies for MSSs. This misarrangement may compel MSSs to use higher power to communicate with the BS and lead to waste the battery power.

Unlike RDCA, MDCA is based on the measurement of actual interference to allocate channels. The BS will scan all channels and selects a proper channel with lowest interference power for channel assignment. This strategy will lead MDCA to use lower frequencies first no matter how far the distance between the BS and MSS is. This behavior will cause a result that more MSSs cannot use lower frequencies as M increasing since lower frequencies run out soon. On the contrary, SDCA allocates appropriate channels for MSSs accord-
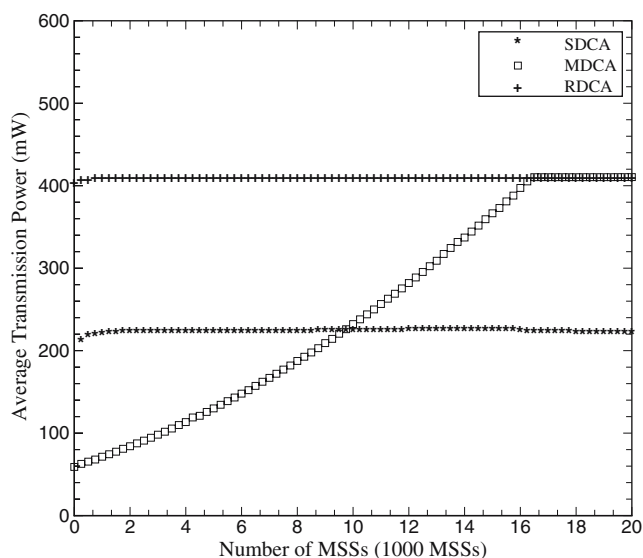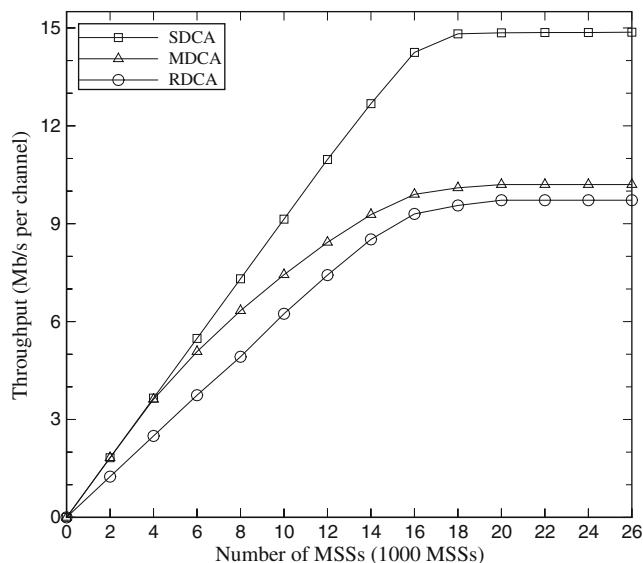

Fig. 13 The comparison of channel throughput derived by SDCA, MDCA, and RDCA under different M

ing to their geographical locations in the macrocell and calculates a minimum transmission power to inform the MSS so that the overall battery consumption can be minimized. This outcome also indicates that the battery consumption can be minimized further if we can get the information of the distance and frequency of the MSS when designing the B3G or 4G systems.

Figure 13 shows the throughput per channel by using SDCA and RDCA, respectively. We can see that both the throughput of SDCA and RDCA increase with increasing M. The throughput of SDCA reaches 14.87 Mb/s per channel (approximately $14.87/15.75 = 94.4\%$ channel utilization deducting the physical and MAC headers) when M reaches 18,000. This is because that SDCA uses a moderate P_t (300 mW) and $f_h(A_h) = 6.675$ GHz to pre-plan the size of macrocell. Therefore, MSSs in the macrocell will be equally distributed into channels and thus the system can get higher through-put. MDCA and RDCA, by contrast, only obtain the throughput of 10.2 Mb/s and 9.72 Mb/s per channel when $M = 20,000$ since they do not allocate channels according to positions. This will lead to higher call blocking ratio due to the limitation of $P_{t,\max}$ and may allocate many MSSs in one channel.

In following simulations, we investigate the relationship between user satisfaction and transmission power by varying M. If the required P_t exceeds the $P_{t,\max}$ of the MSS in the assigned frequency, the MSS will not be served by the BS and leads to call blocking. This result will decrease the user satisfaction. From Fig. 14, we can see that SDCA can achieve 100% user satisfaction when $M \leq 13,000$. The obtained user satisfaction of SDCA outperforms 1.3 times (100%/75.6%) than
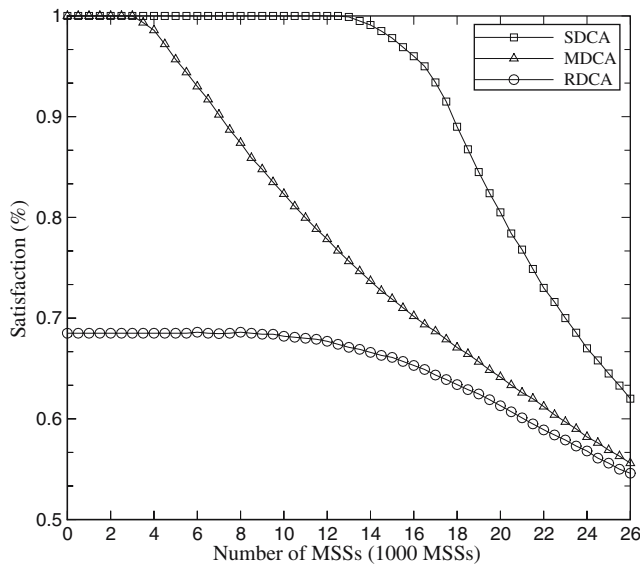

Fig. 12 The average P_t versus M when $\rho = 4$, $B = 5$ MHz, coding rate = 3/4, $SNR_{r,\min} = 24.4$ dB, $F = 7$, $G_t = 16$, $G_r = 18$, $L = 5$ dB

Fig. 14 User satisfaction versus M when $P_{t,\max} = 450$ mW

that of MDCA and 1.49 times (100%/67.1%) than that of RDCA when $M = 13,000$. This is because SDCA allocates adequate channels for MSSs according to the distances between the MSSs and the BS. This strategy enables the BS to allocate channels more equally. On the contrary, MDCA and RDCA does not consider the locations of MSSs and may misarrange frequencies for MSSs. This consequence will lead to inner MSSs competing with outer MSSs in lower frequencies. Thus, outer MSSs will have less chance to get frequencies and cannot communicate with the BS.

In Fig. 15, we reduce the $P_{t,\max}$ from 450 mW to 350 mW to observe the effect on user satisfaction. It
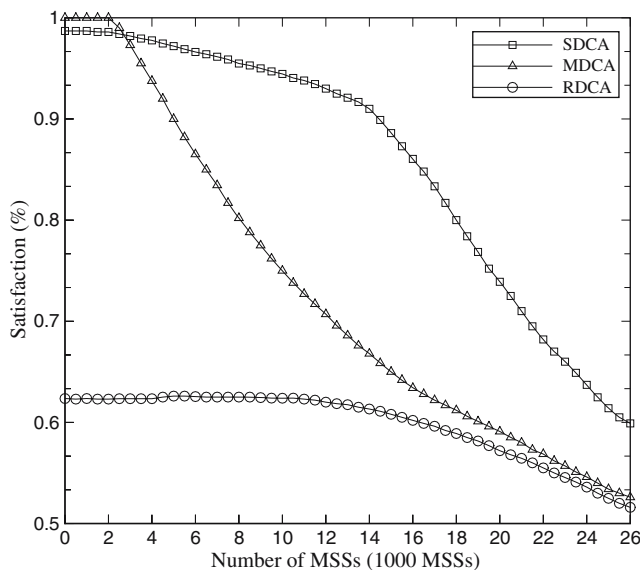
appears an interesting outcome in SDCA when we decrease the $P_{t,\max}$ of MSS. This result shows that SDCA only achieves 98% user satisfaction when $M \leq 3,000$ and is lower than that of MDCA 100%. This is because that the radius is determined by $P_t = 300$ mW and $f_h(A_h) = 6.675$ GHz. However, from Eq. 4.13, the boundary of A_{h-1} needs $P_t > 350$ mW by using $f_h(A_{h-1})$ to achieve this distance. Please notice that, after determining the radius of the macrocell, the boundary of each A_j is determined by jw where w is a fixed value and obtained from Eq. 4.11. This will result in some higher frequencies in A_{h-1} requiring $P_t > 350$ mW. Consequently, SDCA only achieves 98% user satisfaction. However, MDCA uses the measurement strategy to assign channels for MSSs. When M is low, MDCA can achieve 100% user satisfaction since it allocates lower frequencies to MSSs first. But the user satisfaction will drop sharply when $M > 2,000$. Moreover, SDCA can maintain higher user satisfaction about 86% than MDCA and RDCA in 63.4% and 60.2% when $M = 16,000$.

In Figs. 16 and 17, we compare the user satisfaction with M under different $P_{t,\max}$ by using different download/upload links of 2 Mb/s/256 Kb/s, respectively. Comparing Fig. 16 with Fig. 14, we can see that the user satisfaction of SDCA starts degrading from 100% when $M = 8,000$ in Fig. 16 and $M = 12,000$ in Fig. 14. This result $(8,000/12,000 = 2/3)$ can be easily obtained by reversing the ratio of required bandwidth of these two scenarios that 2.25 Mb/s (2 Mb/s + 0.25 Mb/s) over 1.5 Mb/s (0.75 Mb/s + 0.75 Mb/s). This result shows that SDCA can achieve higher user
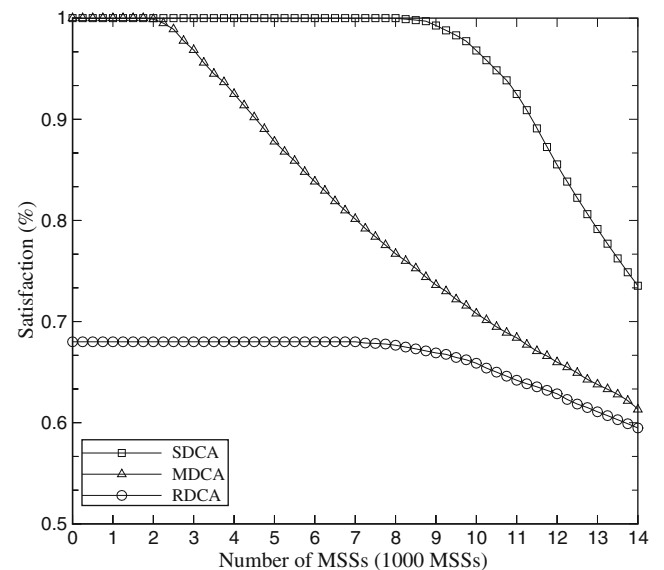

Fig. 15 User satisfaction versus M when $P_{t,\max} = 350$ mW

Fig. 16 User satisfaction versus M when $P_{t,\max} = 450$ mW and DL/UL loads are 2 Mb/s/256 Kb/s
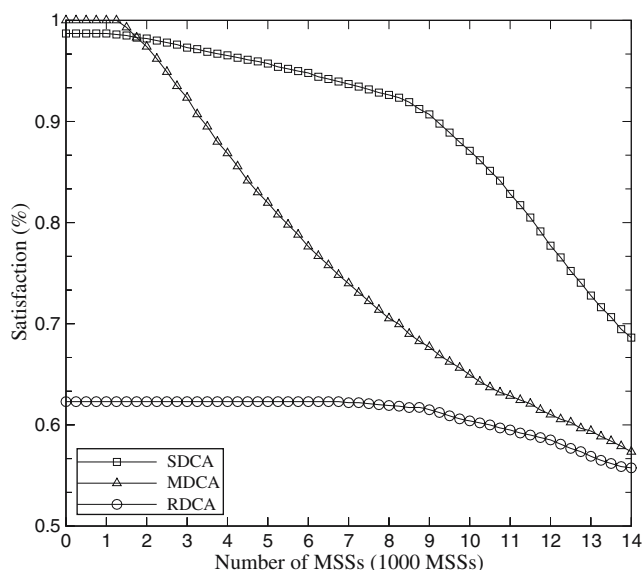
Fig. 17 User satisfaction versus M when $P_{t,max} = 350$ mW and DL/UL loads are 2 Mb/s/256 Kb/s

satisfaction than MDCA and SDCA efficiently even if the required bandwidth of each connection is high.

Figure 18 shows the average P_t of MSS by SDCA, MDCA, and RDCA by increasing M when the spectrum ranges from 2.5–2.69 GHz. SDCA can save 4.59 mW (98.9/103.49 = 95.6%) average P_t compared to RDCA and 4.61 mW (98.9/103.51 = 95.4%) compared to MDCA when $M = 2,500$. We can see that MDCA can obtain lower average transmission power when M is low because MDCA adopts the measured scheme to allocate channels for MSSs. However, the
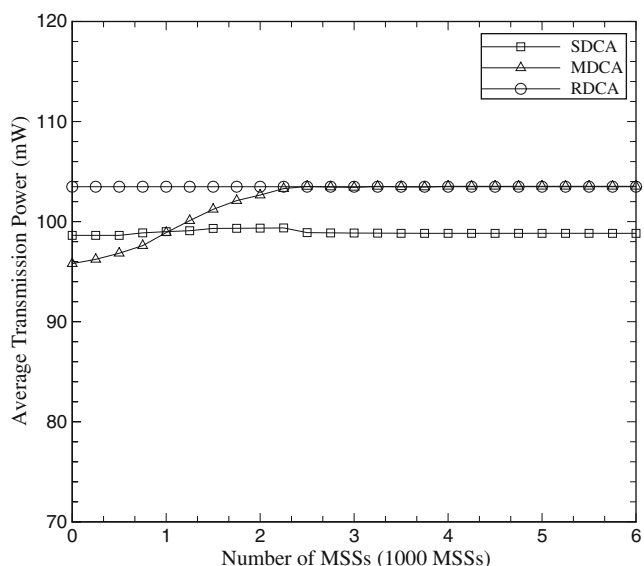
average P_t of MDCA will increase when M increases since no lower frequencies can be allocated for MSSs as M is larger.

In Fig. 19 shows the average P_t of MSS by varying M when the segments of spectrum are 2.5–2.69 GHz and 5.725–5.85 GHz. We can see that, from the result, MDCA can benefit from adding an additional spectrum 5.725–5.85 GHz when M is low. This is because MDCA allocate lower frequencies to MSSs firstly and thus MSSs can use lower P_t to communicate with the BS. However, the superiority of MDCA will degrade when M increases. SDCA, by contrast, obtains a stable power consumption since it allocates channels to MSSs according to MSSs' positions. As the M is large ($M \geq 4,000$), SDCA can save about 66.8% transmission power than MDCA and RDCA. Therefore, from this result, we can know that SDCA can get more remarkable power saving as more frequencies (spectra) can be obtained.

In the following, we investigate the channel utilization of the system when the available spectrum is narrow. Figure 20 shows the obtained throughput from SDCA, MDCA, and RDCA. Compare to Fig. 13, it is obviously that the gap of throughput improvement has been reduced. This is because there are a few channels for selection by SDCA and thus the improvement is limited. However, SDCA still obtains throughput 14.89 Mb/s per channel (approximately 14.89/15.75 = 94.5% channel utilization) than MDCA and RDCA. We can see that SDCA can distribute MSSs into channels efficiently whether the available spectra are wide or narrow.
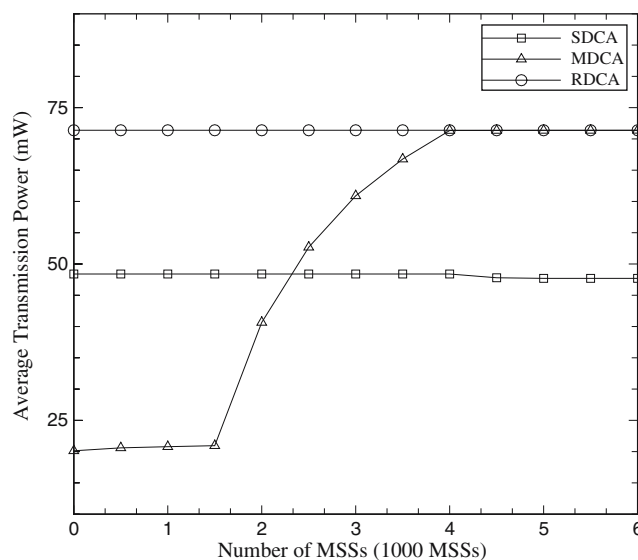

Fig. 18 The average P_t versus M when spectrum is 2.5–2.69 GHz

Fig. 19 The average P_t versus M when spectra are 2.5–2.69 GHz and 5.725–5.85 GHz
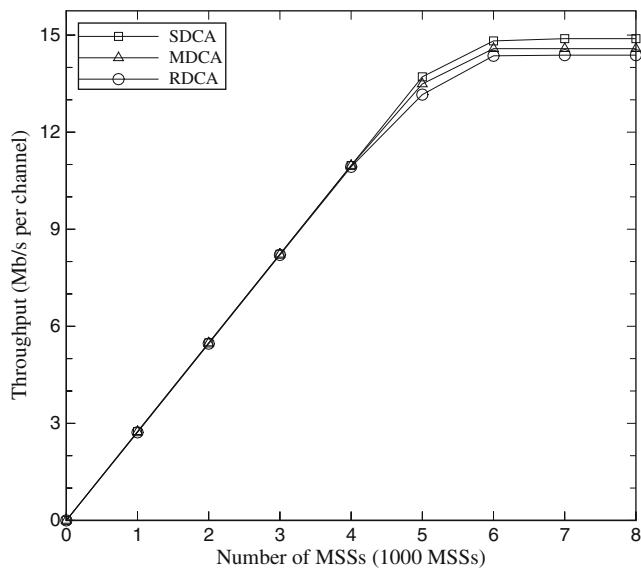
Fig. 20 Throughput versus *M* when spectra are 2.5–2.69 GHz and 5.725–5.85 GHz

Finally, in Fig. 21, we extend the mobility model to vehicular environment. The mobility model uses the random way point model [4] in the macrocell field. Here, each MSS starts its journey from a random location to a random destination with a randomly chosen speed (uniformly distributed between 0 and 20 m/s). Once the destination is reached, another random destination is targeted after a pause. We vary the pause time, which affects the relative speeds of the mobile. In the mobility model, we investigate the out-of-service effect by increasing the mobility. We randomly place $M = 5,000$, $10,000$, and $15,000$ into the macrocell to ob-
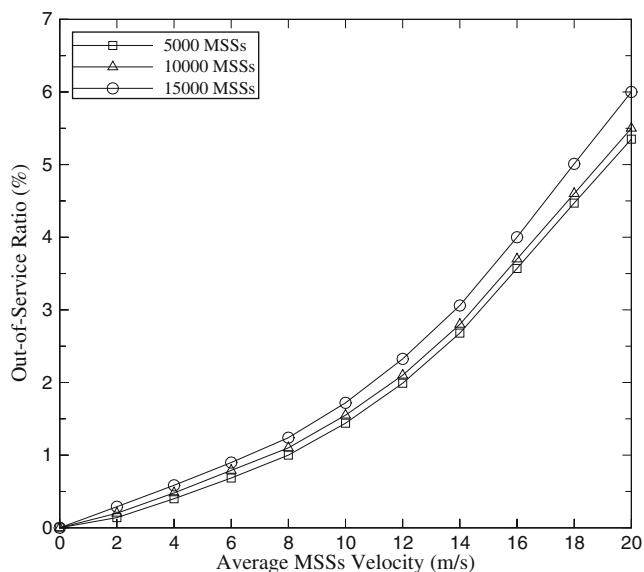
serve the out-of-service effect. We can see that the out-of-service ratio increases with increasing the velocity of the MSS. However, SDCA can control the out-of-service ratio in an acceptable value about 6%. From this result, we can see that SDCA can support mobility well.

6 Conclusion and future work

This paper proposes a signal-aware dynamic channel allocation (SDCA) to improve the channel utilization as well as to reduce the probability of out-of-service for IEEE 802.16 networks. The relationship between the SNR value achieved by different modulation schemes and the maximum transmission distance is also introduced in this paper. According to the received SNR value from the MSS, the BS can estimate the distance from the MSS to the BS and determine an adequate channel for allocation so that the channel is used more efficiently. Moreover, by adopting SDCA, the power consumption of MSSs can be saved further since it tunes minimum transmission powers for MSSs by considering the corresponding geographic locations and allocated channels. Simulation results show that SDCA can achieve the channel utilization (throughput) by up to 94.4%.

To prevent the out-of-service effect on the MSS due to mobility, SDCA uses a location prediction scheme based on measured SNR of REP-REQ messages in each superframe period to prior allocate a new channel for the MSS before it moving out the section. Simulation result shows that the out-of-service ratio gets more improvement when the velocity is high.

As we discussed in Section 4, a longer w will lead to more channels in a section and thus increases the mobility of MSSs and reduces the probability of out-of-service. However, this will lead to lower the enhancement of power saving. This is a tradeoff of the enhancement of power saving and the mobility of the MSSs. How to determine an optimal w considering the mobility and power saving together to improve the system performance is an interesting issue and can be investigated further.

Finally, SDCA still has its limitation that it cannot allocate channels (frequencies) to MSSs dynamically based on adaptive modulation scheme. This is because different modulation schemes correspond to different transmissible range patterns. Thus, how to allocate an appropriate modulation scheme and channel to the MSS according to its location is an interesting issue and future work.

Fig. 21 The out-of-service ratio versus average velocity of MSSs

References

1. Akella MR, Batta R, Delmelle EM, Roger PA, Blatt A, Wilson G (2005) Base station location and channel allocation in a cellular network with emergency coverage requirements. Eur J Oper Res 164(2):301–323

2. Akyildiz IF, Lin YB, Lai WR, Chen RJ (2000) A new random walk model for PCS networks. IEEE J Sel Areas Commun 18(7):1254–1260, July

3. Andersen JB, Rappaport TS, Yoshida S (1995) Propagation measurements and models for wireless communications channels Andersen. IEEE Commun Mag 33(1):42–49, January

4. Broch J et al (1998) A performance comparison of multi-hop wireless ad hoc network routing protocols. In: Proc IEEE/ACM MOBICOM'98, pp 85–97, October

5. Caffery JJ, Stüber GL (1998) Overview of radiolocation in CDMA cellular systems. IEEE Commun Mag 36(4):38–45, April

6. Chatterjee S, Fernando WAC (2004) Blind estimation of channel and modulation scheme in adaptive modulation schemes for OFDM-CDMA based 4G systems. IEEE Trans Consum Electron 50(4):1065–1075, November

7. Chen J, Chen YD (2004) AMNP: ad hoc multichannel negotiation protocol for multihop wireless networks. In: Proc IEEE ICC'2004, Paris, France, vol 6, pp 3607–3612, June

8. Chen J, Sheu ST (2005) Distributed multichannel MAC protocol for IEEE 802.11 ad hoc wireless LANs. Comput Commun 28(9):1000–1013, June

9. Cheng MML, Chuang JCI (1996) Performance evaluation of distributed measurement-based dynamic channel assignment in local wireless communications. IEEE J Sel Areas Commun 14(4):698–710, May

10. Chu T-S, Greenstein LJ (1999) A quantification of link budget differences between the cellular and PCS bands. IEEE Trans Veh Technol 48(1):60–65, January

11. Eklund C et al (2002) IEEE standard 802.16: a technical overview of the wirelessman air interface for broadband wireless access. IEEE Commun Mag 40(6):98–107, June

12. Erceg V et al (1999) An empirically based path loss model for wireless channels in suburban environments. IEEE J Sel Areas Commun 17(7):1205–1211, July

13. Erceg V et al (1999) A model for the multipath delay profile of fixed wireless channels. IEEE J Sel Areas Commun 17(3):399–410, March

14. Evci C, Fino B (2001) Spectrum management, pricing, and efficiency control in broad-band wireless communications. In: Proc IEEE 89(1):105–115, January

15. Fong B, Ansari N, Fong ACM, Hong GY, Rapajic PB (2004) On the scalability of fixed broadband wireless access network deployment. IEEE Commun Mag 42(9):1–12, September

16. Ghosh A, Wolter DR, Andrews JG, Chen R (2005) Broadband wireless access with WiMax/802.16: current performance benchmarks and future potential. IEEE Commun Mag 43(2):129–136, February

17. Hui SY, Yeung KH (2003) Challenges in the migration to 4G mobile systems. IEEE Commun Mag 41(12):54–59, December

18. IEEE 802.16 Working Group (2004) IEEE standard for local and metropolitan area networks–part 16: air interface for fixed broadband wireless access systems. IEEE Std. 802.16-2004, October

19. IEEE 802.16 Working Group (2003) Part 16: air interface for fixed broadband wireless access systems–amendment 2: medium access control modifications and additional physical layer specifications for 2-11 GHz. IEEE Std 802.16a, April

20. IEEE 802.16 Working Group (2004) Draft amendment to IEEE standard for local and metropolitan area network–part 16: air interface and mobile broadband wireless access systems. IEEE Std 802.16e/Draft 2, April

21. Jain M (2005) Channel allocation policy in cellular radio network. Appl Math Model 29(1):65–83, January

22. Jianfeng W, Tho LN, Yinglin X (2004) ZCZ-CDMA and OFDMA using M-QAM for broadband wireless communications. Wirel Commun Mob Comput 4(4):427–438, June

23. Jingwen N, Nahrstedt K (2004) QoS specification languages for distributed multimedia applications: a survey and taxonomy. IEEE Multimed 11(3):74–87, July

24. Kavak A, Torlak M, Vogel WJ, Xu G (2000) Vector channels for smart antennasaXMeasurements, statistical modeling, and directional properties in outdoor environments. IEEE Trans Microwave Theor Tech 48(6):930–937, June

25. Koffman I, Roman V (2002) Broadband wireless access solutions based on OFDM access in IEEE 802.16. IEEE Commun Mag 40(4):96–103, April

26. Laroia R, Uppala S, Junyi L (2004) Designing a mobile broadband wireless access network. IEEE Signal Process Mag 21(5):20–28, September

27. Leaves P et al (2004) Dynamic spectrum allocation in composite reconfigurable wireless networks. IEEE Commun Mag 42(5):72–81, May

28. Mandal S, Saha D, Mahanti A (2004) A real-time heuristic search technique for fixed channel allocation (FCA) in mobile cellular communications. Microprocess Microsyst 28(8):200–211, October

29. Michalski A, Czajewski J (2004) The accuracy of the global positioning systems. IEEE Instrum Meas Mag 7(1):56–60, March

30. Munoz M, Rubio CG (2004) A new model for service and application convergence in B3G/4G Networks. IEEE Wirel Commun 11(5):6–12, October

31. Pabst R et al (2004) Relay-based deployment concepts for wireless and mobile broadband radio. IEEE Commun Mag 42(9):80–89, September

32. Pätzold M, Youssef N (2001) Modelling and simulatoin of dierctoin-selective and frequency-selective mobil radio channels. Int J Electron Commun 55(6):433–442, December

33. Plitsis G (2003) Coverage prediction of new elements of systems beyond 3G: the IEEE 802.16 system as a case study. In: Proc IEEE VTC 2003-Fall, Orlando, FL, vol 4, pp. 2292–2296, October

34. Rappaport TS (1996) Wireless communications: principles and practice, Prentice hall, Upper Saddle, NJ

35. Sharma P, Perry E, Malpani R (2003) IP multicast operational network management: design, challenges, and experiences. IEEE Network 17(2):9–55, March

36. Tseng YC, Chao CM, Wu SL, Sheu JP (2002) Dynamic channel allocation with location awareness for multi-hop mobile ad hoc networks. Comput Commun 25(7):676–688, May

37. Wang YT, Sheu JP (2004) A dynamic channel-borrowing approach with fuzzy logic control in distributed cellular networks. Simulation Modelling Practice and Theory 12(3–4):287–303, July

38. Wong SH, Wassell LJ (2002) Channel allocation for broadband fixed wireless access. In: Proc IEEE WPMC'02, Honolulu, Hawaii, vol 2, pp 626–630, October
39. Wongthavarawat K, Ganz A (2003) Packet scheduling for QoS support in IEEE 802.16 broadband wireless access systems. Int J Commun Syst 16(1):81–96, February
40. Yousef NR, Sayed AH, Jalloul LMA (2003) Robust wireless location over fading channels. IEEE Trans Veh Technol 52(1):117–126, January
41. Verdone R, Zanella A, Zuliani L (2005) Performance of a cellular network based on frequency hopping with dynamic channel allocation and power control. IEEE Trans Wirel Commun 4(1):46–56, January

Wei-Kuang Tan was born in Taipei on October 25, 1979. He received the B.S. degree in the Department of Computer Science, Tamkang University and M.S. degree in the Department of Computer Science, Chang Gung University, Taiwan, R.O.C, in 2003 and 2005, respectively. Currently, he is a software engineer in Portwell Technology Corporation. His research interests include design, analysis, and implementation of network protocols, wireless communications, and embedded systems. Mr. Tan is a student member of the IEEE.

Jenhui Chen received his B.S. and Ph.D. degrees in Computer Science and Information Engineering (CSIE) from Tamkang University in July 1998 and January 2003, respectively. In the spring of 2003, he joined the faculty of Computer Science and Information Engineering Department at Chang Gung University and served as the Assistant Professor. Dr. Chen served as the referee for several famous international journals including *IEEE Transactions on Fuzzy Systems*, *IEEE Transactions on Mobile Computing*, *IEEE Transactions on Wireless Communications*, *IEEE Transactions on Parallel and Distributed Systems*, *IEEE Transactions on Computers*, and *ACM Mobile Networks and Applications* (*MONET*). He served as a Program Committee Member for the 2005 IEEE International Conference on Parallel and Distributed Systems and a referee for the 2005 IEEE/RSJ International Conference on Intelligent Robots and Systems. His main research interests include design, analysis, and implementation of communication and network protocols, wireless networks, robotics, artificial intelligence, and bioinformatics. He is a member of IEEE and IEICE.
E-mail: jhchen@mail.cgu.edu.tw